AIP | Review of Scientific Instruments

Measurement of dispersion relation of waves in a tandem mirror plasma by the Fraunhofer-diffraction method

A. Mase, J. H. Jeong, A. Itakura, K. Ishii, and S. Miyoshi

Citation: Review of Scientific Instruments **61**, 1247 (1990); doi: 10.1063/1.1141219
View online: http://dx.doi.org/10.1063/1.1141219
View Table of Contents: http://scitation.aip.org/content/aip/journal/rsi/61/4?ver=pdfcov
Published by the AIP Publishing

Measurement of dispersion relation of waves in a tandem mirror plasma by the Fraunhofer-diffraction method

A. Mase, J. H. Jeong, A. Itakura, K. Ishii, and S. Miyoshi

Plasma Research Center, University of Tsukuba, Tsukuba 305, Japan

(Received 18 August 1989; accepted for publication 19 December 1989)

The Fraunhofer diffraction measurements from a tandem mirror plasma are reported. The successful use of a new multichannel detector array permits a detailed study of $\mathbf{k}-\omega$ spectra of long-wavelength waves with a few plasma shots. The observed dispersion relations are in good agreement with those of drift wave including a Doppler shift due to $\mathbf{E}\times\mathbf{B}$ rotation velocity.

INTRODUCTION

Considerable interest has been focused on the study of low-frequency waves, since they are thought to be the main cause of the anomalous transport and energy loss in magnetically confined plasmas. A measurement of spatially and temporally resolved frequency (ω) and wave number (k) spectra is essential for the waves. Microwave to infrared laser scattering techniques have been used for the purpose.[1-5]

In a scattering experiment, the frequency spectrum is obtained by frequency analysis of the scattered wave. The wave number spectrum, on the other hand, is obtained by varying the scattering angle using the Bragg relation $k=2k_i\sin(\theta_s/2)$, where k_i is the incident wave number and θ_s is the scattering angle. The scattering angle has to be larger than the divergence angle of the incident beam in order to avoid stray light. The divergence angle $\Delta\theta$ is given by

$$\Delta\theta \simeq 2/k_i a_0, \tag{1}$$

where $2a_0$ is the incident beam diameter measured at the $1/e^2$ power points. The Bragg relation and Eq. (1) yield the wave number resolution for small angle scattering as

$$\Delta k \simeq 2/a_0. \tag{2}$$

New techniques of the opposite limit, called "far-forward scattering"[6] and "Fraunhofer-diffraction method"[7] have been presented, where the scattered wave is heterodyne detected with the undeviated incident beam, thus detected within the divergence of the probing beam. This technique offers a means of investigating long-wavelength waves, which are considered to be more relevant to the anomalous transport.

The present article contains a description of the first application of the Fraunhofer-diffraction (FD) method to the tandem mirror GAMMA 10. In Sec. I, a brief review of the FD theory is described. This is followed by a description of the experimental apparatus in Sec. II. Section III gives experimental results and discussion on an identification of the waves.

I. REVIEW OF THE FD THEORY

In this section a brief review of the FD method is given together with a summary of the relevant equations.

Let an incident beam of Gaussian mode travel in the z direction and a plasma wave propagate in the x direction. The plasma wave is assumed to exist at the distance of z_0 from the beam waist of the incident beam.

When a linearly polarized incident wave with the electric field of

$$\mathbf{E}_i=\mathbf{E}_0\Psi_i(x,y,z)\exp j(\omega_i t-\mathbf{k}_i\cdot\mathbf{r}) \tag{3}$$

is diffracted by an electron density fluctuation given by

$$\tilde{n}_e(x,y,z)=\tilde{n}_{e0}\exp[-(y^2+z^2)/r_p^{\,2}]\cos(kx-\omega t'), \tag{4}$$

the electric field of the scattered wave at the observing point $Q(R_0)$ is given by

$$\mathbf{E}_s=\mathbf{E}_0 r_0\int\frac{1}{R}\Psi_i(x,y,z)\tilde{n}_e \times\exp j(\omega_i t'-\mathbf{k}_i\cdot\mathbf{r})dV, \tag{5}$$

where Ψ_i is the normalized spatial distribution function of the incident beam, r_p is the width of the plasma wave, t' is the retarded time, r_0 is the classical electron radius, R is the distance between a diffraction point and the observing point $Q(R_0)$, and V is the diffracting volume.

Assuming the Gaussian profile of Ψ_i, the FD intensity profile of an oscillating component is calculated by[7]

$$\begin{aligned}I_{\rm ac}&=|\mathbf{E}_s^*\mathbf{E}_f+\mathbf{E}_s\mathbf{E}_f^*|/2\\&=|A|^2(1/q^2)\tilde{n}_{e0}e^{-u^2}\\&\quad\times(e^{-(u-\theta)^2}\sin\{\rho[u^2-(u-\theta)^2]+\omega t\}\\&\quad+e^{-(u+\theta)^2}\sin\{\rho[u^2-(u+\theta)^2]-\omega t\}),\end{aligned} \tag{6}$$

where $\mathbf{E}_f$ is the electric field of the undeviated incident beam at the observing point, $|A|^2=2E_0^2\pi^{3/2}r_0w_0^2Z_r^2/R_0w_f$, $q=2Z_r/r_p$, $Z_r=k_iw_0^2/2$ is the Rayleigh zone calculated for the plasma beam waist w_0, $u=x_f/w_f$ is the x coordinate normalized by the spot size at the front focal plane, $\rho=z_0/Z_r$, and $\theta=kw_0/2$ is the normalized wave number.

It is shown that $I_{\rm ac}$ is maximum at $u=\theta/2(=u_m)$ for $\theta\gg 1$ and wave number of a plasma wave can be directly determined by measuring u_m for each frequency component. When $\theta\lesssim 1$, k is obtained by the curve fitting between a measured profile and theoretical one, since the above-mentioned method gives a poor k resolution. If the density fluctuations are at the beam waist in the plasma and the FD profile is measured in the detector position z_f relative to the front focal plane of a receiving lens, the FD profile is given by replacing θ to $\theta_f[=(w_f/w_s)\theta]$ and ρ to $\rho_f[=(z_f/z_0)(Z_r/Z_{rf})\rho]$ in Eq. (6),[8] where w_s is the spot size of the

 0034-6748/90/041247-04$02.00

beam on the observation plane and Z_{rf} $(=k_i w_f^2/2)$ is the Rayleigh zone calculated for the front focal plane beam waist.

II. EXPERIMENTAL APPARATUS

A. GAMMA 10 device

The details of the tandem mirror GAMMA 10 are shown in elsewhere.[9,10] End plugging experiments are carried out with a combination of neutral beam injection and microwave heating. Four 28 GHz, 100 kW gyrotrons are used to generate mirror-confined hot electrons that produce a thermal barrier potential depression ($\omega = 2\omega_{ce}$ ECRH) and warm electrons for positive potential peak ($\omega = \omega_{ce}$ ECRH) that confines central cell ions. The central cell plasma is heated with 200 kW of ion cyclotron resonance frequency (ICRF) power.

At each end, radially and azimuthally segmented plates are installed which can be biased in order to control the potential distribution as well as floated through a 1-MΩ resistor. In the standard operation of GAMMA 10, the end plates are floated so that the net current to the ends is effectively zero. The potentials at the central cell, Φ_c and barrier midplane, Φ_B are measured with gold neutral beam probes,[11] and plug one, Φ_p is determined by the energy analysis of multigridded type end-loss analyzers (ELAs). The density profiles are also measured with movable interferometers.

B. The instruments of FD system

A schematic of the FD apparatus is illustrated in Fig. 1. The apparatus is located at the central cell of GAMMA 10, that is, 2.4 m from the center toward a mirror throat. The output of a Gun oscillator ($P_0 \simeq 100$ mW, $f = 45$ GHz) is focused to the center of the plasma by a fused-quartz lens. Beam profile measurement indicates a focal spot radius of $w_0 \simeq 33$ mm at the e^{-2} power point. The frequency-shifted FD signal and the unshifted transmitted wave are focused via another lens onto the beam-lead GaAs Schottky barrier diodes bonded to gold bowtie antennas[12] which are monolithically fabricated on a fused-quartz substrate of 25×25 mm^2. The rectangular waveguide antennas in TE_{10} mode are installed to the reverse side of the diode detectors, i.e., the substrate side. The aperture of the waveguide antenna is 4.78×2.39 mm^2. The beam width at the observation plane is 14 mm. The aperture is selected to be smaller than the beam width. The FD signals at four points are measured in one shot. The detector array can also be moved in order to study the FD profiles in detail.

Since the Rayleigh zone at the beam waist in the plasma exceeds 520 mm, while the plasma radius is less than 140 mm, the density fluctuations are effectively localized at the beam waist. The antennas are located at $z_f = 60$ mm from the front focal plane. This corresponds in Rayleigh zone to be $Z_{rf} = 92$ mm and yields $\rho_f = z_f/Z_{rf} = 0.65$. This displacement of the slit from the front focal plane is found to be useful for an accurate wave number determination by a curve fitting of the theoretical profiles with the measured ones.

The down-converted IF signal by mixing of diffracted wave and undeviated transmitted wave is amplified by a chain of low noise amplifiers. The amplified signal is fed into

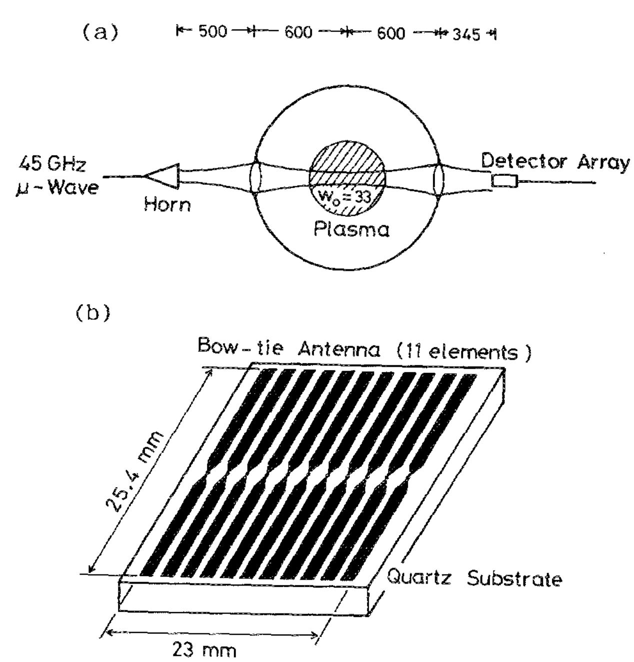

FIG. 1. Schematic of the FD apparatus. (a) Optical system, (b) detector array.

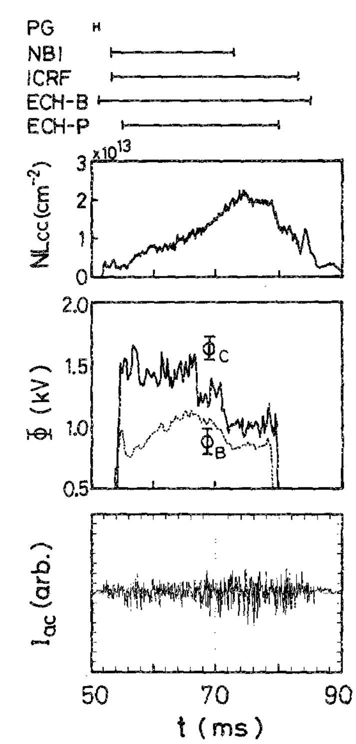

FIG. 2. Time evolution of the central-cell line-density, potentials at the central cell and barrier midplane, and the FD signal obtained with one of the detectors.

a #2264 LeCroy waveform recorder. A personal computer analyzes the waveform recorder signals by calculating the fast Fourier transformation.

III. EXPERIMENTAL RESULTS AND DISCUSSION

A. Determination of $k-\omega$ spectra

The time evolution of the plasma parameters is shown in Fig. 2 together with time sequence of the heating systems: from top to bottom, the central cell line density, the potentials at the central cell and barrier midplane, and the FD signal obtained with one of the detectors. When the fundamental ECRH (plug-ECRH) is applied, the end-loss fluxes decrease associated with the formation of the thermal barrier and plug potentials. The FD signal increases with increasing the line density. The signal is Fourier analyzed in every 2.5 or 5 ms.

The frequency spectra at four FD points can be obtained in one plasma shot. Usually, 12 FD points are enough to determine the FD profile at fixed frequency, which means that three plasma shots are necessary to obtain the dispersion relation of waves. The FD profiles for various values of frequency obtained at $t = 65$ ms are shown in Fig. 3. The solid lines shown in Fig. 3 are calculated from Eq. (6). From the best fitting between the experimental value and theoretical value, we can determine the wave number $k_\perp$ of the density fluctuations.

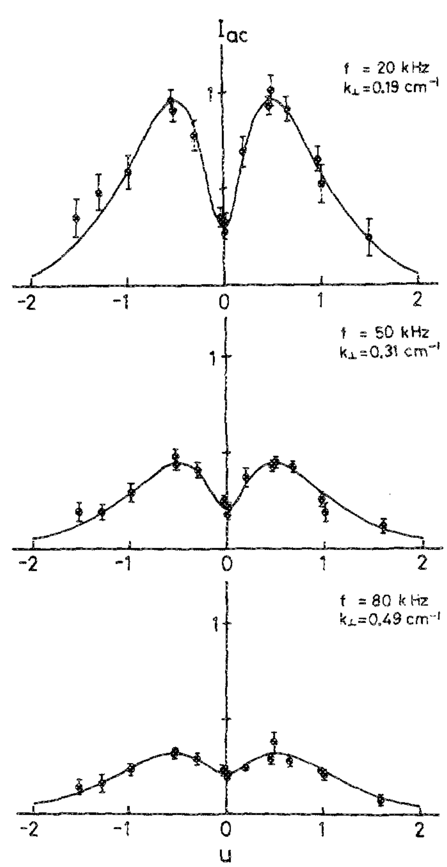

FIG. 3. FD profiles for various values of frequency.

B. Dispersion relations of low-frequency wave

Examples of the observed dispersion relations are shown in Fig. 4 for various values of plug-ECRH power. The values of phase velocity $v_p = \omega/k_\perp$ obtained from Fig. 4 are shown in Table I. During the plug ECRH is applied, the plasma potential increases as shown in Fig. 2. This causes the plasma rotation due to $\mathbf{E}\times\mathbf{B}$ drift. The rotation velocity is given by

$$v_r = E_r/B, \tag{7}$$

where $E_r = -\partial\Phi_c(r)/\partial r$. Therefore, the effect of a Doppler shift due to the rotation velocity is included in the phase velocity v_p of the observed wave; thus, we obtain

$$v_p = \omega/k_\perp = |v_d - v_r|. \tag{8}$$

From the following features of experimental observations, we may conclude that the density fluctuations are drift wave mode, that is, the values of frequency and wave number are in the range of drift wave, and the density fluctuations are localized at the region of the maximum density gradient. The electron diamagnetic drift velocity is given by

$$v_d = \frac{\kappa T_e}{eBL_n}\frac{1}{1+k_\perp^2\rho_s^2}, \tag{9}$$

where κ is the Boltzmann constant, e is the charge of an electron, T_e is the electron temperature, B is the magnetic field, $L_n = -n_e/(\partial n_e/\partial r)$ is the density scale length, $\rho_s = (m_i\kappa T_e/e^2B^2)^{1/2}$, and m_i is the ion mass. The values of v_r and v_d calculated from Eqs. (7) and (9) are shown in Table I. The measured profiles of the density and potential as well as T_e and B are used for the calculations. A satisfactory agreement between the two values, v_p and $|v_d - v_r|$, is obtained. The agreement is confirmed for various plasma potentials of both well type and hill type.

IV. SUMMARY

The millimeter wave FD apparatus was designed to measure density fluctuations in the central-cell plasma of

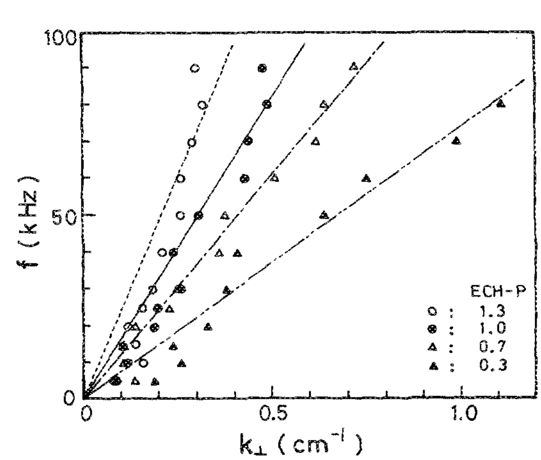

FIG. 4. Dispersion relations of the density fluctuations for various values of plug-ECRH power. The value (1.0) corresponds to the output power of about 80 kW.

TABLE I. Values of v_r, v_d, and v_p for various values of plug-ECRH power.

ECH	Φ_c (V)	E_r (kV/m)	v_r (m/s)	v_d (m/s)	v_p (m/s)
0.3	900 ± 100	7.0 ± 0.9	$8.7 \pm 1.1 \times 10^3$	$2.3 \pm 0.7 \times 10^3$	5.5×10^3
0.7	1100 ± 150	8.7 ± 1.2	10.9 ± 1.5	2.9 ± 0.9	7.9
1.0	1300 ± 150	10.2 ± 1.2	12.8 ± 1.5	3.1 ± 0.9	10
1.3	1600 ± 200	12.8 ± 1.6	16.0 ± 2.0	3.2 ± 0.7	13

GAMMA 10. A new multichannel detector was developed for the measurements. A combination of a waveform digitizer and a personal computer system gives an analysis of frequency spectra at the four FD points simultaneously. Thus, the capability of wave dispersion measurement with a few discharges is demonstrated via the observation of naturally occurring long-wavelength waves of $k_\perp = 0.1$–1.0 cm^{-1}. Such a regime of $k_\perp$ cannot be measured using a conventional Thomson scattering. The dispersion relations are developed for various plasma conditions. The direct measurement of potential profiles using beam probes enables the first quantitative confirmation of the Doppler shifted drift wave model. It is also noted that the importance of $\mathbf{E} \times \mathbf{B}$ rotation effects on fluctuations has been recognized recently since the poloidal rotation due to the radial electric field has been observed during the time of L to H transition in tokamaks. It is considered that the poloidal flow reduces the fluctuations and leads to increased plasma confinement.

ACKNOWLEDGMENTS

The authors deeply acknowledge the GAMMA 10 group of University of Tsukuba for their collaboration. They would also like to thank Professor Muraoka and Dr. Matsuo of Kyushu University for their useful discussions, and Dr. Harada and his group of Sanyo Electric Co., Ltd., Semiconductor Research Center for supplying the detector.

[1]E. Mazzucato, Phys. Rev. Lett. **48**, 1828 (1982).
[2]C. M. Surko and R. E. Slusher, Phys. Rev. Lett. **37**, 1747 (1976).
[3]A. Semet, A. Mase, W. A. Peebles, N. C. Luhmann, Jr., and S. J. Zweben, Phys. Rev. Lett. **45**, 445 (1980).
[4]T. Tetsuka, A. Nishizawa, T. Sakai, K. Kawahata, A. Mase, T. Tsukishima, and J. Fujita, J. Phys. Soc. Jpn. **52**, 1242 (1983).
[5]D. L. Brower, W. A. Peebles, and N. C. Luhmann, Jr., Nucl. Fusion **27**, 2055 (1987).
[6]D. E. Evans, M. von Hellermann, and E. Holzhauer, Plasma Phys. **24**, 819 (1982).
[7]Y. Sonoda, Y. Suetsugu, K. Muraoka, and M. Akazaki, Plasma Phys. **25**, 1113 (1983).
[8]D. E. Evans, E. J. Doyle, D. Frigione, M. von Hellermann, and A. Murdoch, Plasma Phys. **25**, 617 (1983).
[9]M. Inutake, T. Cho, M. Ichimura, K. Ishii, A. Itakura, Y. Kiwamoto, Y. Kusama, A. Mase, S. Miyoshi, Y. Nakashima, T. Saito, A. Sakasai, K. Sawada, I. Wakaida, N. Yamaguchi, and K. Yatsu, Phys. Rev. Lett. **55**, 939 (1985).
[10]A. Mase and GAMMA 10 Group, Invited Lecture at the Course on Basic and Advanced Fusion Plasmas Diagnostic Techniques, International School of Plasma Physics, Varenna, **3**, 913 (1986).
[11]K. Ishii, M. Kotoku, T. Segawa, I. Katanuma, A. Mase, and S. Miyoshi, Rev. Sci. Instrum. **60**, 3270 (1989).
[12]D. B. Rutledge and M. S. Muha, IEEE Trans. **AP-30**, 535 (1982).